



Salvia miltiorrhiza Bunge (Danshen) and Bioactive Compound Tanshinone IIA Alleviates Cisplatin-Induced Acute Kidney Injury Through Regulating PXR/NF- κ B Signaling

OPEN ACCESS

Edited by:

Jianping Chen,
Shenzhen Traditional Chinese
Medicine Hospital, China

Reviewed by:

Liang Ma,
Sichuan University, China
Hongwei Gao,
Guangxi University of Chinese
Medicine, China
Ryota Shizu,
University of Shizuoka, Japan

*Correspondence:

Yue-Yu Gu
guyy@gzucm.edu.cn
Xu-Sheng Liu
liuxsheng@gzucm.edu.cn

[†]These authors have contributed
equally to this work

Specialty section:

This article was submitted to
Renal Pharmacology,
a section of the journal
Frontiers in Pharmacology

Received: 22 January 2022

Accepted: 24 February 2022

Published: 24 March 2022

Citation:

Dou J-Y, Zhang M, Cen H, Chen Y-Q,
Wu Y-F, Lu F, Zhou J, Liu X-S and Gu
Y-Y (2022) *Salvia miltiorrhiza* Bunge
(Danshen) and Bioactive Compound
Tanshinone IIA Alleviates Cisplatin-
Induced Acute Kidney Injury Through
Regulating PXR/NF- κ B Signaling.
Front. Pharmacol. 13:860383.
doi: 10.3389/fphar.2022.860383

Jing-Yun Dou^{1†}, Min Zhang^{1†}, Huan Cen², Yi-Qin Chen¹, Yi-Fan Wu¹, Fuhua Lu¹,
Jiuyao Zhou³, Xu-Sheng Liu^{1*} and Yue-Yu Gu^{1,3*}

¹Department of Nephrology, Guangdong Provincial Hospital of Chinese Medicine, The Second Affiliated Hospital of Guangzhou University of Chinese Medicine, Guangzhou, China, ²Department of Ultrasound, The Second Affiliated Hospital of Guangzhou University of Chinese Medicine, Guangzhou, China, ³Department of Pharmacology, School of Pharmaceutical Sciences, Guangzhou University of Chinese Medicine, Guangzhou, China

Objective: The present study aims to provide evidence on the potential protective role of *Salvia miltiorrhiza* Bunge (Danshen) and its bioactive compound Tanshinone IIA (TanIIA) in AKI and to reveal the specific regulatory function of PXR/NF- κ B signaling in AKI-induced renal inflammation.

Methods: A network pharmacological analysis was used to study target genes and regulatory networks in the treatment of *Salvia miltiorrhiza* on AKI. Further experiments with *in vivo* AKI mouse model and *in vitro* studies were applied to investigate the renal protective effect of TanIIA in AKI. The mechanisms of TanIIA regulating PXR/NF- κ B signaling in renal inflammation were also studied.

Results: Network pharmacology had suggested the nuclear receptor family as new therapeutic targets of *Salvia miltiorrhiza* in AKI treatment. The *in vivo* studies had demonstrated that TanIIA improved renal function and inflammation by reducing necrosis and promoting the proliferation of tubular epithelial cells. Improved renal arterial perfusion in AKI mice with TanIIA treatment was also recorded by ultrasonography. *In vitro* studies had shown that TanIIA ameliorated renal inflammation by activating the PXR while inhibiting PXR-mediated NF- κ B signaling. The results had suggested a role of PXR activation against AKI-induced renal inflammation.

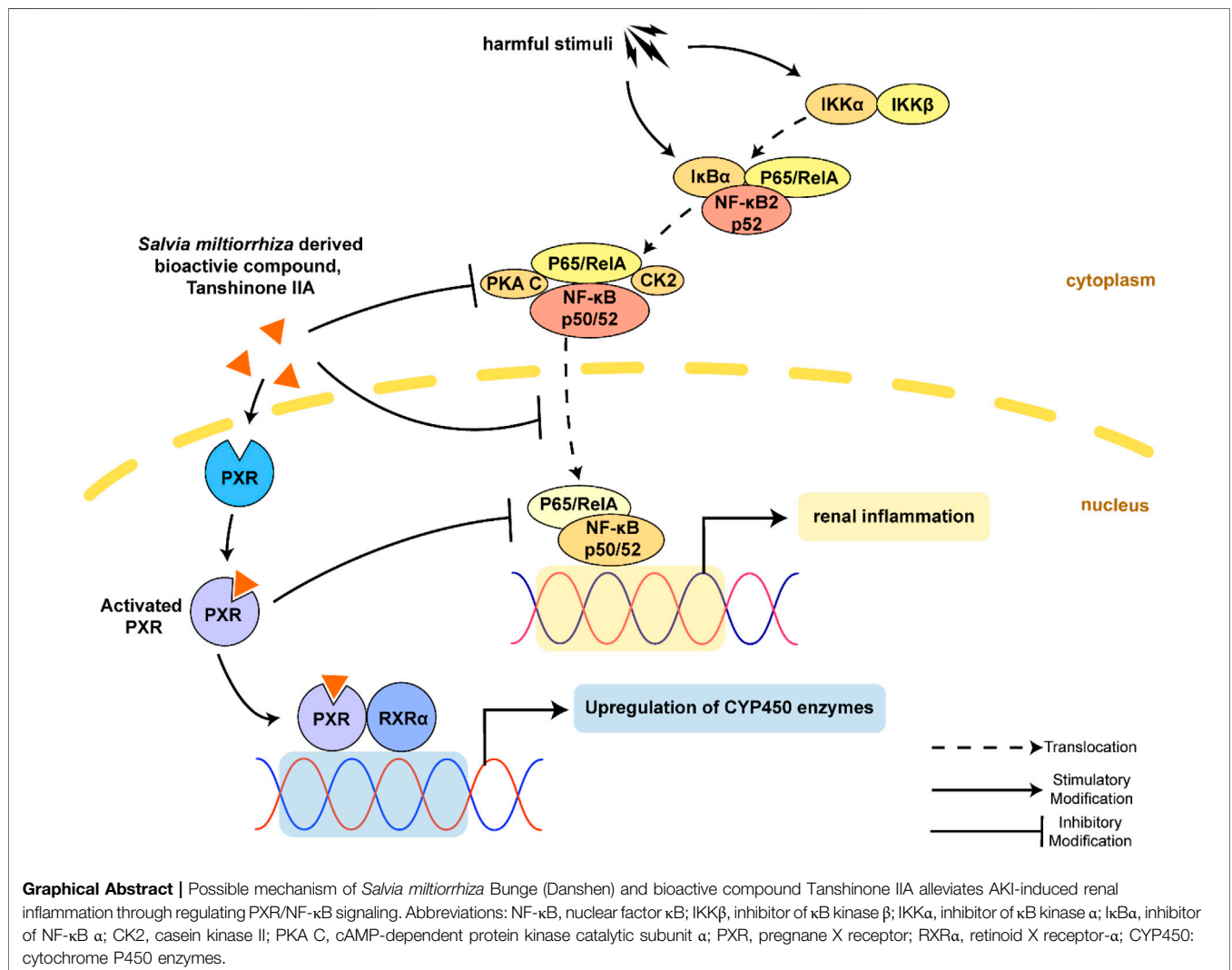
Conclusion: *Salvia miltiorrhiza* Bunge (Danshen) may protect the kidneys against AKI by regulating nuclear receptors. TanIIA improved cell necrosis proliferation and reduced renal inflammation by upregulating the expression of the PXR and inhibiting NF- κ B signaling in a PXR-dependent manner. The PXR may be a potential therapeutic target for AKI treatment.

Keywords: acute kidney injury, pregnane X receptor, NF- κ B, *Salvia miltiorrhiza*, tanshinone IIA, renal inflammation

INTRODUCTION

Acute kidney injury (AKI) involves a rapid decline in renal function within hours to days. It is a global burden with a high mortality rate that exceeds breast cancer, heart failure, or diabetes so far (Kellum et al., 2021). Approximately 15% of patients in hospital, and more than 57% of patients in the intensive care unit (ICU) develop AKI. (Hoste et al., 2015; Scholz et al., 2021). Nowadays, treatment and therapies for AKI vary, depending on the cause of kidney injuries and preventing complications until the kidneys recover. The initial renal insults may induce the infiltration of inflammatory leukocytes within the glomerulus and tubulointerstitial area. Unresolved renal inflammation can impair the function of the nephrons and lead to a reduction in the estimated glomerular filtration rate (eGFR) (Gu et al., 2021). We are now clear that renal inflammation is the central pathogenic mechanism that drives AKI. However, the mechanisms of renal inflammation are not fully elaborated, and practical strategies and therapeutic drugs are still limited.

The pregnane X receptor (PXR, NR1I2) is a well-known member of the nuclear receptor superfamily (He et al., 2017). The PXR functions as a ligand-activated transcription factor to upregulate the activity and expression of drug-metabolizing enzymes (i.e., phase I oxidative enzymes: cytochrome P450 (CYP450) enzymes), conjugating enzymes (phase II enzyme such as glutathione S-transferase, GST), and transporters (phase III transport uptake and ATP-dependent efflux pump such as multidrug resistance protein 1, MDR1). These enzymes are key mediators in regulating detoxification and clearance of xenobiotics. The PXR contains a DNA-binding domain (DBD) and a ligand-binding domain (LBD) connected by a hinge region. The LBD is a mostly hydrophobic flexible pocket for a wide range of drugs and compounds. The PXR then forms a transcriptionally active complex with retinoid X receptor α (RXRα) and binds to the DNA response elements to control gene expression associated with xenobiotic and endobiotic metabolism. The PXR can be activated by a wide range of endogenous and exogenous ligands such as hormone metabolites, bile acids, and drugs (Hogle et al., 2018); it also acts as a key player in inflammation, energy



metabolism, and endocrine homeostasis (Oladimeji and Chen, 2018).

In humans, the PXR is mainly expressed in the liver, intestine, and kidneys. As for the kidneys, the proximal tubular epithelial cells (TECs) express the PXR at a relatively high level. A variety of studies have highlighted the significant role of the PXR in renal toxicity, diabetic nephropathy, and chronic kidney disease (CKD) (Velenosi et al., 2014; Lee et al., 2018; Watanabe et al., 2018). Nuclear factor κ B (NF- κ B) is a protein complex that controls an extensive array of genes in immune response evoked by harmful cellular stimuli. The NF- κ B signaling acts as a significant determinant for the progression of renal inflammatory pathogenesis of AKI (Markó et al., 2016; Song et al., 2019). Interestingly, previous studies on inflammatory bowel disease and liver inflammation had demonstrated the suppressing effect of the PXR on NF- κ B activity (Deuring et al., 2019; Okamura et al., 2020), suggesting the anti-inflammatory effect of the PXR. However, the mechanisms of the PXR on NF- κ B-induced renal inflammation and therapies are still lacking.

Salvia miltiorrhiza Bunge (Danshen) is a perennial plant that is highly valued for its roots in traditional Chinese medicine. Tanshinones are critical lipophilic diterpenoids from Danshen extracts. These secondary metabolites are essential resources derived from medicinal plants (Ma et al., 2015). Among tanshinones, TanIIA is the most abundant compound that exerts anti-inflammatory effects in various diseases (Guo et al., 2020). Moreover, TanIIA was reported to be an PXR activator and induce the transcriptional level of cytochrome P450 3A4 (CYP3A4) (Yu et al., 2009; Liu et al., 2011). Mechanistic studies have revealed the anti-inflammatory effect of TanIIA through PXR activation (Zhang et al., 2015a; Zhang et al., 2015b; Zhu et al., 2017).

Based on previous findings, we hypothesized that *Salvia miltiorrhiza* and its active component, TanIIA, may protect the kidneys against AKI by regulating the PXR/NF- κ B signaling in renal inflammation. A network pharmacological analysis was applied to investigate target genes and regulatory networks modulated by *Salvia miltiorrhiza*. Moreover, we elucidated the protective effects and underlying mechanisms of TanIIA on AKI *in vivo* and *in vitro*. A molecular docking study was also applied to reveal the possible drug-protein interaction mode of TanIIA and PXR. The present study provides novel aspects on the anti-inflammation effect of *Salvia miltiorrhiza* and reveals a role of the PXR/NF- κ B signaling pathway in AKI. PXR may serve as one of the promising therapeutic targets against AKI-induced inflammation.

MATERIALS AND METHODS

Prediction of *Salvia miltiorrhiza*-Associated Target Genes, Their Intersection on AKI, and Analysis on Gene Ontology (GO) and Enrichment KEGG pathways

A network pharmacological analysis was applied to study related genes in treating *Salvia miltiorrhiza* on AKI. We searched the keyword “Danshen” in the Traditional Chinese Medicine Systems Pharmacology Database and Analysis Platform (TCMSP [\[tcmsp.com/tcmssp.php\]\(http://tcmsp.com/tcmssp.php\)\) \(Ru et al., 2014\) to obtain active ingredients and their ADME \(absorption, distribution, metabolism, and excretion\) information. OB \(oral bioavailability\) and DL \(drug-likeness\) were recorded. The criteria of OB \$\geq\$ 30% and DL \$\geq\$ 0.18 suggest that the ingredients with good absorption into blood were screened as potential active ingredients. Then, the corresponding target proteins of the active ingredients were collected from the TCMSP database, and corresponding target genes were analyzed *via* String database \(Von Mering et al., 2003\) UniProt databases \(The UniProt Consortium, 2018\). The target genes of AKI were obtained from the GeneCards \(<https://www.genecards.org/>\), OMIM \(<https://omim.org/>\), and DisGeNET database \(<https://www.disgenet.org/>\). We used the Venn online analysis tool \(<https://www.omicsshare.com/>\) to study the intersection target genes of *Salvia miltiorrhiza* and AKI. These genes are considered potential targets of *Salvia miltiorrhiza* for treating AKI. With those intersection target genes, we performed GO and KEGG pathway enrichment analyses by using the ClueGO plug-in of Cytoscape 3.6.0. The screening was based on \$p < 0.01\$ and a \$\kappa\$ score \$\geq 0.53\$ to visualize the results of GO and KEGG enrichment \(Bindea et al., 2009\). A flowchart of network pharmacology study is shown in **Supplementary Figure S3**. The original data in the network pharmacological analysis are available on Figshare \(<https://doi.org/10.6084/m9.figshare.17895506.v1>\)](http://</p>
</div>
<div data-bbox=)

Animal Model of Cisplatin-Induced AKI and TanIIA Treatment

TanIIA and cisplatin were HPLC-purified products purchased from Sigma-Aldrich. The chemical structure of TanIIA was constructed by ChemOffice (CambridgeSoft, Cambridge, MA) as shown in **Figure 7A**. TanIIA was dissolved in 150 μ l saline with 0.01% DMSO. Male C57BL/6 mice at eight weeks of age (weighting 20–25 g) were housed under $23 \pm 2^\circ\text{C}$, $55 \pm 5\%$ humidity, and 12/12-hour light/dark cycle environment with free access to water and food. The number of mice was calculated and assigned to groups following an allocation process (Charan and Kantharia, 2013; Beshpalov et al., 2020). The mice were divided into 4 groups ($n = 5$): normal control (CTRL), AKI model, AKI+TanIIA12.5 (12.5 mg/kg/day, *i.p.*) low-dose treatment, and AKI+TanIIA25 (25 mg/kg/day, *i.p.*) high-dose treatment group. The doses were chosen based on previous publications (Jiang et al., 2015; Zhang et al., 2020). The AKI treatment groups received a single cisplatin injection (20 mg/kg, *i.p.*). CTRL received the same volume of control saline intraperitoneally. The body weight of all mice was recorded before and after 72 h of the cisplatin injection. The mice were killed on AKI day 3. Serum, kidneys, and other organs were collected after ultrasonic assessment for renal blood flow. The experimental protocol was approved by the Institutional Animal Care and Use Committee of Guangdong Provincial Hospital of Chinese Medicine (Approval No. 2020020).

Arterial Ultrasonography and Renal Function

Renal ultrasonography was performed to visualize renal blood vessels using a high-frequency ultrasound imaging system (Vevo

2100, Visual Sonics Inc., Toronto, Canada) as previously described (Okumura et al., 2018). All measurements were done on the right abdomen. Peak systolic and end-diastolic blood flow velocities (mm/s) were measured in the renal artery to obtain the pulsatility index (PI). An experienced technician who was blinded to the study protocol repeated the measurement three times. According to the manufacturer's instructions, serum creatinine was measured with commercial kits (C011-2-1, Nanjing Jiancheng Bioengineering Institute, China).

Cell Culture and Cytotoxicity Assay

Human proximal tubular cell line HK-2 was purchased from American Type Culture Collection (CRL-2190, ATCC, VA, United States). HK-2 cells were cultured in DMEM/F12 medium supplemented with 10% (v/v) FBS (Gibco, United States) under a humidified atmosphere with 5% CO₂ at 37°C. Cells were trypsinized and harvested when the confluence reached 80–90%.

Cytotoxicity activity was assayed by using a Cell Counting Kit-8 (CCK-8) (Dojindo, Japan) according to the manufacturer's instructions. Dimethyl sulfoxide (DMSO) was used as the vehicle and did not exceed 0.1%. Each cell line would be seeded into a new flask and treated with 5% DMEM/F12 medium with DMSO (0.1% v/v) and TanIIA at different concentrations. HK-2 cells were, respectively, seeded into 96-well plates at a density of 5×10^3 cells/well, and cultured in the DMEM/F12 with a low FBS concentration for 24 h. Then they were divided into control groups, DMEM/F12 with DMSO (0.1% v/v) (100 μ l/well) and TanIIA group at various final concentrations of 3.125, 6.25, 12.5, 25, 50, and 100 μ M (100 μ l/well). After incubating for 6, 12, and 24 h, the medium was replaced with 10 μ l 10% CCK-8 solution dissolved in 90 μ l PBS, and all the cells were incubated for another 1 h at 37°C in the dark. Absorbance at 450 nm was measured using a Sunrise™ Microplate Reader (TECAN, Switzerland). Each concentration was repeated five times in the same plate, and all experiments were performed at least three times. The percentage of cell viability was normalized to control group cells to calculate the inhibition rate:

Inhibition rate (IR) (%) = 1

$$- \frac{\text{Sample solution OD value}}{\text{Control OD value}} \times 100\%.$$

IC₅₀ was calculated with the Excel add-in tool ED50plus (created by Mario H. Vargas, MD).

Gene Silencing of PXR

In total, 1×10^6 HK-2 cells were transfected with the hPXR small-interfering RNA (siRNA) or the control siRNA (Santa Cruz Biotechnology, CA, United States) using Lipofectamine 3000 transfection reagent (Thermo Fisher Scientific Inc., United States) according to the manufacturer's instructions. The control siRNA was used as a negative control. RIF (rifampin) (Sigma-Aldrich, United States) (10 μ M) was used as the positive control. Cells were treated with DMSO (0.1% v/v), RIF (10 μ M), and TanIIA (5 μ M) and were stimulated with/without TNF- α (20 ng/ml) for 24 h. The cells were then subjected to the NF- κ B luciferase reporter assay.

PXR Transactivation Reporter Assay and PXR-Mediated NF- κ B Reporter Assay

The pSG5-hPXR expression plasmids and pGL3-CYP3A4-XREM luciferase reporter construct, containing the basal promoter (−10466/+53) with the proximal PXR response element (ER6) and the distal xenobiotic responsive enhancer module (XREM, −7836/−7208) of the CYP3A4 gene 5'-flanking regions inserted to pGL3-basic reporter vector, were kind gifts from Dr. Sridhar Mani (Albert Einstein College of Medicine, Bronx, NY, United States) (Huang et al., 2007). The pRL-TK *Rotylenchulus reniformis* control vector was purchased from Promega, Madison, United States.

HK-2 cells were seeded at 60–70% confluence into opaque 96-well plates at a density of 1×10^5 cells/well in DMEM/F12 containing 10% FBS and cultured for 12 h. The cells were transiently transfected with pGL3-CYP3A4-XREM, pSG5-hPXR nuclear receptor expression vector, and pRL-TK control vector in a particular ratio with Lipofectamine 3000 transfection reagent according to the manufacturer's instructions. After 6 h of incubation, the transfected HK-2 cells were exposed to TanIIA at 1, 2.5, 5, and 10 μ M; RIF (10 μ M); and control (0.1% DMSO) for an additional 24 h. Following the treatments, HK-2 cells were rinsed with PBS, and the luciferase activities were determined using a Dual-Luciferase Reporter Assay System (Promega, Madison, United States) and an Infinite F500 multimode microplate reader (TECAN, Switzerland).

HK-2 cells were transiently transfected with pGL4.32 [luc2P/NF- κ B-RE/Hygro] NF- κ B reporter, pCMV6-entry or pCMV6-XL4-hPXR, and pRL-TK (Promega, Madison, United States) with Lipofectamine 3000 transfection reagent according to the manufacturer's instructions. After overnight transfection, the cells were treated as control (0.1% DMSO), TanIIA (5 μ M), and RIF (10 μ M) for 24 h, and additional incubation with/without TNF- α (20 ng/ml) for another 24 h. A standard dual luciferase assay was performed on cell lysates and detected using an Infinite F500 multimode microplate reader.

Transfection efficiency was expressed as fold induction of firefly to *Renilla* luciferase activities relative to control. Each concentration of the test substances was repeated five times in the same plate, and the transfection experiments were performed at least three times. Data are expressed as mean \pm SEM from three independent experiments.

Histology and Immunohistochemistry

Tissues were fixed with 4% buffered paraformaldehyde for 48 h, and they were cut into 3- μ m paraffin sections for hematoxylin and eosin (HE), periodic acid–Schiff (PAS) and Masson's trichrome staining. The morphology of renal tubules with prominent necrosis were recorded. Patchy or diffuse denudation with loss of brush border detachment of cells with intratubular cast formation was identified. The degree of tubular injury was scored as score 0: no tubular injury; score 1: \leq 10% tubules injured; score 2: 11–25% tubules injured; score 3: 26–50% tubules injured; score 4: 51–74% tubules injured; and score 5: \geq 75% tubules injured.

Immunohistochemistry (IHC) sections were de-waxed and proceeded by a microwave-based antigen retrieval technique following previous procedures (Gu et al., 2018). Antibodies used in IHC included PCNA Rabbit mAb IKK β Rabbit mAb (Cell Signaling Technology, MA, United States), anti-NF- κ B p105/p50 Rabbit mAb (Abcam, MA, United States). The kidney sections were stained with primary and secondary antibodies. The sections were developed with diaminobenzidine (DAB) to produce a brown color. The percentage of positive staining areas of PCNA, NF- κ B p105/p50, and IKK β expression was measured by ImageJ software (NIH, Bethesda, MD, United States).

Immunofluorescence Staining

HK-2 cells were seeded, incubated, and treated with 0.1% DMSO, TanIIA (5 μ M), and/or TNF- α (20 ng/ml) for 24 h. Cells were fixed with 4% paraformaldehyde for 30 min, permeabilized with 0.5% Triton X-100 for 20 min, and blocked with 5% BSA for 30 min at room temperature. Primary antibodies against NF- κ B p65 (1:100, Cell Signaling Technology, MA, United States) were incubated with cells at 4°C overnight. After washing with PBS three times, an FITC-conjugated secondary antibody was added for 60 min at room temperature. All slides were mounted with DAPI-containing mounting medium and then analyzed with a fluorescence microscope (Leica Microsystems, Wetzlar, Germany).

ELISA

Mouse serum was collected and centrifuged at 3,000 rpm for 15 min at 4°C. The level of neutrophil gelatinase-associated lipocalin (NGAL), IL-6, and TNF- α in blood was detected by using ELISA kits (R&D Systems Inc., Minneapolis, United States), following the manufacturer's instructions.

RNA Extraction and Real-Time PCR

Total RNA was isolated from the kidney tissue with the TRIzol reagent (Thermo Fisher Scientific Inc., United States) according to the manufacturer's protocol. Total RNA was quantified by the absorbance ratio (260/280 nm) and reverse-transcribed into cDNA using PrimeScript™ RT reagent (Takara Bio Inc., Japan). All the PCR reactions were carried out using SYBR® Premix EX Taq™ II Kit (Takara Bio Inc., Japan) in 96-well optical plates on an ABI ViiA™ 7 PCR System (Applied Biosystems, Thermo Fisher Scientific, United States). The quantity of each transcript was calculated as described in the instrument manual and normalized to the housekeeping gene β -actin. The ratio of target to β -actin was calculated as $\Delta C_t = C_t(\text{target}) - C_t(\beta\text{-actin})$, ratio (target) = $2^{-\Delta\Delta C_t}$. The primers used for real-time PCR are listed in **Supplementary Table S5**.

Western Blot Analysis

The proteins from renal cortical tissues were extracted with RIPA lysis buffer. The samples were subjected to Western blot analysis with primary antibodies against phospho-NF- κ B p65, NF- κ B p65, IKK β , NF- κ B p105/p50 (Cell Signaling Technology, MA, United States), RXR α (Abcam, MA,

United States), PXR, and GAPDH (Santa Cruz Biotechnology, CA, United States) overnight at 4°C and subsequently incubated with the conjugated secondary antibody of horseradish peroxidase-labeled anti-rabbit IgG or anti-mouse IgG (Cell Signaling Technology, MA, United States) at room temperature. Target protein expression was detected by using an Image Lab System (Bio-Rad Laboratories Inc., Hercules, CA, United States) and analyzed with ImageJ software.

Molecular Docking

The ligand and the receptor recognize each other and bind together by geometry and energy matching. Molecular docking provides new insights into the ligand–receptor interactions and structural features of the two molecules within the active site. To predict the protein–ligand interaction, we performed the CDOCKER algorithm and Libdock module in Discovery Studio (DS) 2.5 (Accelrys Software Inc., San Diego, United States) to evaluate the potential interaction of ligands and the proteins, respectively. The 3D crystal structure of TanIIA (CID: 164676) was obtained from the PubChemProject (<http://pubchem.ncbi.nlm.nih.gov/compound/>). The receptor PXR was selected from Protein Data Bank (PDB) (<http://www.rcsb.org/pdb/>). The program was run by using a localhost9943 server on Microsoft Windows 7.

The calculation of root mean square deviation (RMSD) was carried out. RMSD indicates the reliability of the results from the above modules. Docking procedures on DS 2.5 were as follows: the water molecules in the targeted protein PXR were removed, and the hydrogen atoms were added. Then, PXR and the ligand were refined with CHARMM. The active sites of PXR were defined automatically according to the internal ligand binding site through a series of algorithms by DS2.5. A three-dimensional pharmacophore model of the ligand with the targeted protein was generated in the CDOCKER module and Libdock module.

Statistical Analysis

Data are expressed as mean \pm SEM. All data were analyzed with GraphPad Prism 5 (GraphPad Software, San Diego, CA) by one-way analysis of variance (ANOVA) for single-variable analysis or two-way ANOVA for two independent variables, followed by Turkey's multiple comparisons test. Student's *t*-test was used for paired data.

RESULTS

Prediction of Potential Targets and Signaling Pathways of *Salvia miltiorrhiza* Treatment in AKI

Overall, 65 eligible active ingredients (**Supplementary Table S1**) and 139 target proteins (**Supplementary Table S2**) were collected from TCMSP. Among these proteins, 133 significant target genes were collected from the String and Uniprot database (**Supplementary**

Table S3); 7123 AKI-related target genes were collected from GeneCards, OMIM, and DisGeNET databases; and 122 intersection genes (**Supplementary Table S4, Supplementary Figure S1**) of *Salvia miltiorrhiza* and AKI were screened out by the Venn analysis tool. A total of 15 KEGG pathways were enriched, as shown in **Supplementary Figure S2**. A total of 22 GO pathways were enriched. **Figure 1A** has indicated the pathways associated with *Salvia miltiorrhiza* treatment in AKI. The numbers of the target genes in the pathway were also highlighted. A pie chart was used to classify 22 GO pathways into 7 significant signaling pathways and percentage of genes related to AKI (as shown in **Figure 1B**): nuclear receptor activity (4.55%), extrinsic apoptotic signaling pathway (4.55%), response to alkaloid (13.64%), integral component of synaptic membrane (27.27%), regulation of blood vessel diameter (13.64%), regulation of smooth muscle cell proliferation (22.73%), and neurotransmitter biosynthetic process (13.64%) (**Figure 1zc C**).

Among these pathways, we put great interest in the process of nuclear receptor activity. The nuclear receptor family has shown a percentage of 19.3% association on *Salvia miltiorrhiza* treatment in AKI with 11 target genes involved (AKR1B1, AR, CYP1A1, ESR1, ESR2, NR1H2, NR3C1, PGR, PPARG, RXRA, and STAT3). Up to date, the underlying mechanisms of how nuclear receptors, especially PXR, affect kidney injury are still poorly understood. Following this clue, we tried to reveal the role of PXR in AKI *in vivo* and *in vitro* and seek an alternative possibility in developing *Salvia miltiorrhiza* as a renal protective drug.

TanIIA Improves Renal Function by Alleviating Renal Injury in Cisplatin-Induced AKI

On AKI day 3, the bodyweight of both AKI model and AKI+TanIIA25 (mg/kg/day) was significantly decreased compared to the CTRL group (**Figure 2A**). As shown in **Figure 2B**, serum creatinine levels were increased in all cisplatin-treated groups compared to CTRL. However, the creatinine level was reduced in both TanIIA treatment groups compared with the cisplatin-induced AKI model. The neutrophil gelatinase-associated lipocalin (NGAL) and kidney injury molecule-1 (KIM-1) are important biomarkers related to AKI (Schrezenmeier et al., 2017). Consistent with the creatinine results, the serum and mRNA levels of NGAL (**Figures 2C,D**) and mRNA of KIM-1 were significantly reduced by the TanIIA treatment compared to the AKI model (**Figure 2E**).

Morphological changes of renal damage were shown by HE and PAS staining. Tubular damages such as tubular dilation, atrophy, cast formation, and sloughing of TECs, or loss of the brush border in cisplatin-treated groups were observed (marked as arrowheads and asterisks). TanIIA reduced tubular necrosis, restored the brush border, and formed fewer casts in the tubule, therefore alleviating tubular injuries in a dose-dependent manner compared to the AKI group (**Figure 3A**). Masson's trichrome staining indicated an improvement in fibrosis in TanIIA treatment groups, with less collagen formation within the renal interstitial area (**Figure 3B**). IHC staining has shown an increased staining area of PCNA (cell proliferation marker) in

both TanIIA treatment groups compared to the AKI model (**Figure 3C**).

TanIIA Activates Increases Arterial Blood Flow and Constrains NF- κ B-Induced Renal Inflammation

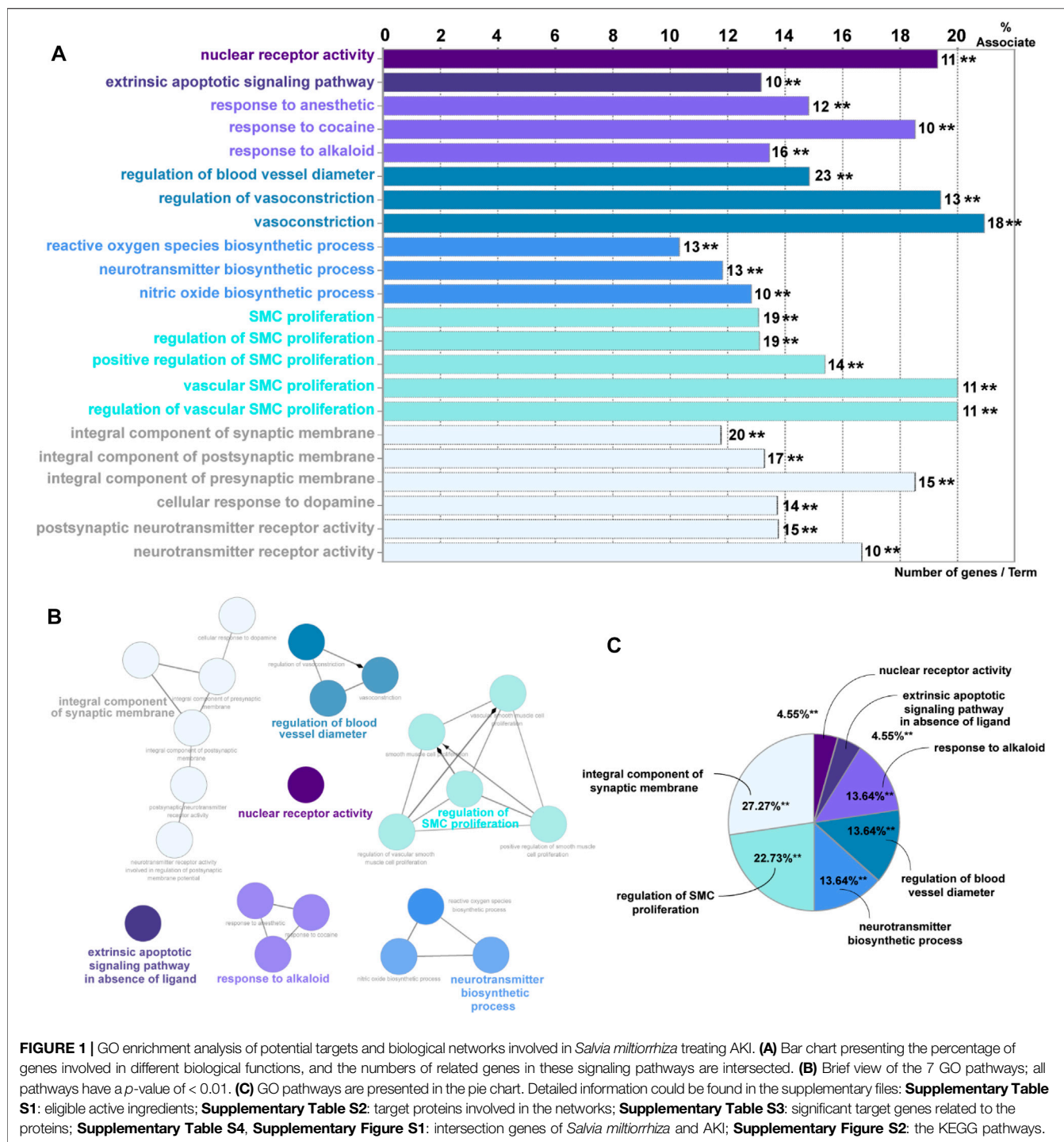
It is well-demonstrated that AKI may lead to endothelial dysfunction and impaired vascular autoregulation, which causes vasoconstriction and changes renal hemodynamics. Therefore, the reduction in medullary blood flow can be observed in AKI (Ozkok and Edelstein, 2014). Ultrahigh-frequency ultrasound is a non-invasive and sensitive method that helps monitor renal function. The color Doppler and pulsed wave Doppler images could be used to show renal blood supply and arterial flow velocity patterns (Kelahan et al., 2019). In the present study, renal ultrasonography was used to observe renal blood flow at AKI day 3. The upper panel in **Figure 4A** has shown the representative image, showing the anatomical relationship of renal vein and artery in normal mouse kidneys. The color Doppler-based sonographic assessment had shown an increase in the pulsatility index (PI) in the AKI model, while PI of the TanIIA treatment was decreased compared to the AKI group (**Figure 4B**). The results had indicated better renal perfusion in TanIIA-treated mice under AKI conditions.

To investigate how TanIIA affects renal inflammation, we hypothesize that TanIIA inhibits the activation of the NF- κ B-activated inflammatory response. Therefore, the expressions of key mediators in NF- κ B signaling were measured. The expression of NF- κ B p105/p50 and IKK β was significantly reduced by TanIIA treatment when compared to the AKI model (**Figures 4C–E**), and the results were confirmed by the NF- κ B p105/p50 and IKK β protein expression measured by Western blot (**Figures 4K–M**). Similarly, serum levels of pro-inflammatory cytokines in kidneys, such as TNF- α and IL-6, mRNA level of IL-1 β , and TGF- β were also declined in TanIIA treatment groups compared to the AKI model (**Figures 4F–J**). These findings had suggested an anti-inflammatory effect of TanIIA in AKI by inhibiting the production of pro-inflammatory cytokines and the activation of NF- κ B signaling.

TanIIA Human and Mouse PXR and Inhibits PXR-Mediated NF- κ B Activity

We studied the mechanisms of TanIIA that affected the PXR/NF- κ B signaling pathway in AKI mouse and human TEC cell line HK-2. The expression level of mouse PXR and RXR α was significantly decreased in the kidneys by cisplatin treatment (**Figures 5A–C**). TanIIA treatment significantly induced the expression of mouse PXR, coactivator RXR α , and expression of cytochrome P3A11 (*Cyp3a11*, mouse homolog of CYP3A4). On the other hand, TanIIA suppressed the activation of NF- κ B signaling by inhibiting the phosphorylation of NF- κ B p65 (**Figure 5D**). Moreover, reduced mRNA expression of mouse PXR and downstream *Cyp3a11* were also observed in AKI mouse kidneys, while TanIIA treatment upregulated the mRNA expression of mouse PXR and *Cyp3a11* significantly compared to the AKI model (**Figures 5E,F**).

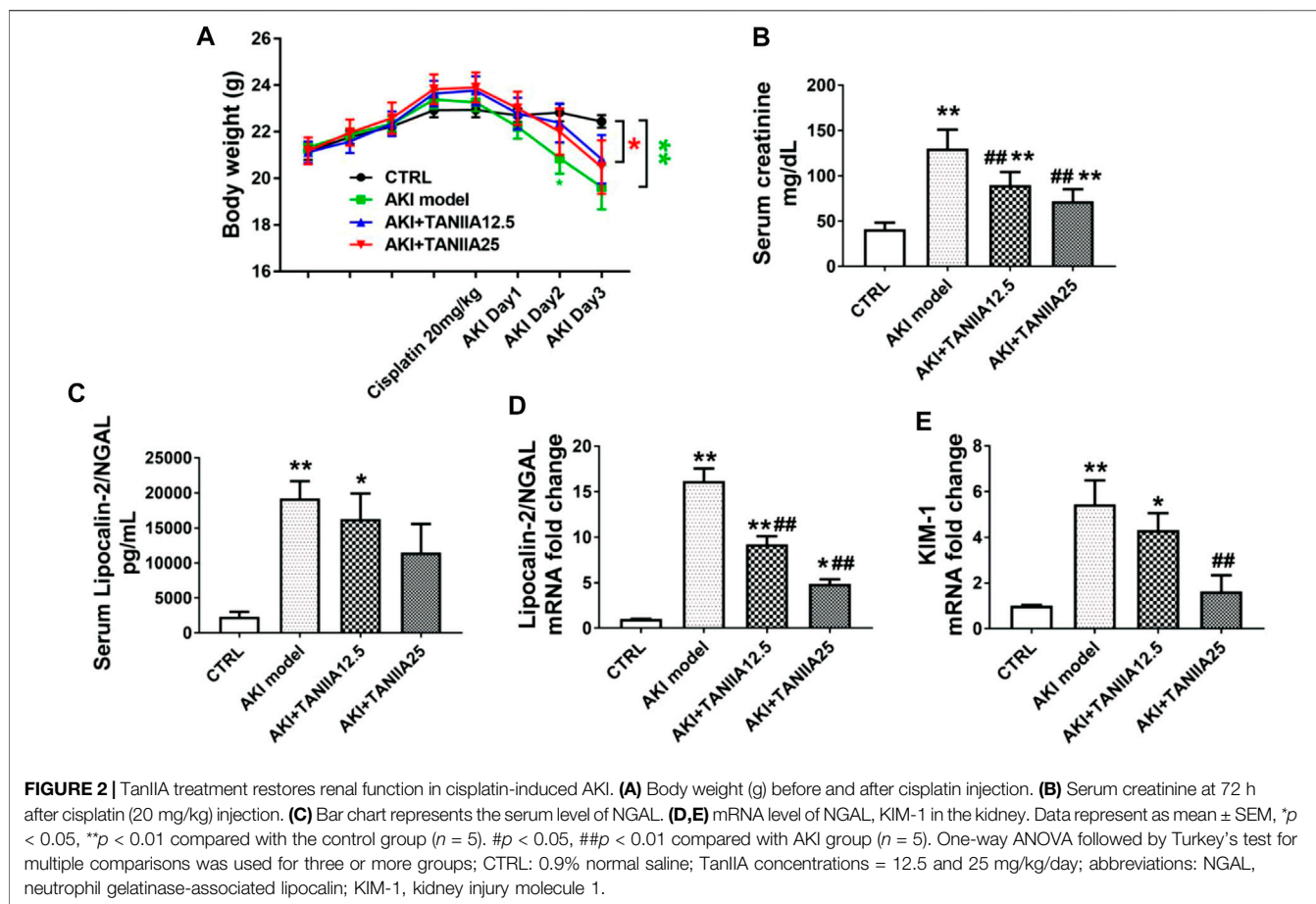
A transfection luciferase reporter assay was performed in HK-2 cells to evaluate the effect of TanIIA on human PXR and



PXR-mediated CYP3A4 transcription activity. The optimal concentration for TanIIA was chosen by cell viability assay. The IC₅₀ values for TanIIA in HK-2 cells were 17.16 ± 1.83 μM (6 h) (Figure 6A). HK-2 cells were transiently transfected with pGL3-CYP3A4-XREM, pSG5-hPXR nuclear receptor expression vector and pRL-TK control vector to investigate whether TanIIA could transcriptionally activate human PXR-mediated CYP3A4 expression. A strong hPXR agonist, rifampin

(RIF = 10 μM), was used as the positive control. Cells were incubated with/without TanIIA at different concentrations (TanIIA = 1, 2.5, 5, 10 μM). TanIIA activated human PXR and induced CYP3A4 promoter activity (Figure 6B). We confirmed the optimal concentration of TanIIA (5 μM) to the activation of human PXR.

To explore the role of human PXR on the repression of NF-κB by TanIIA, HK-2 cells were transfected with hPXR small-



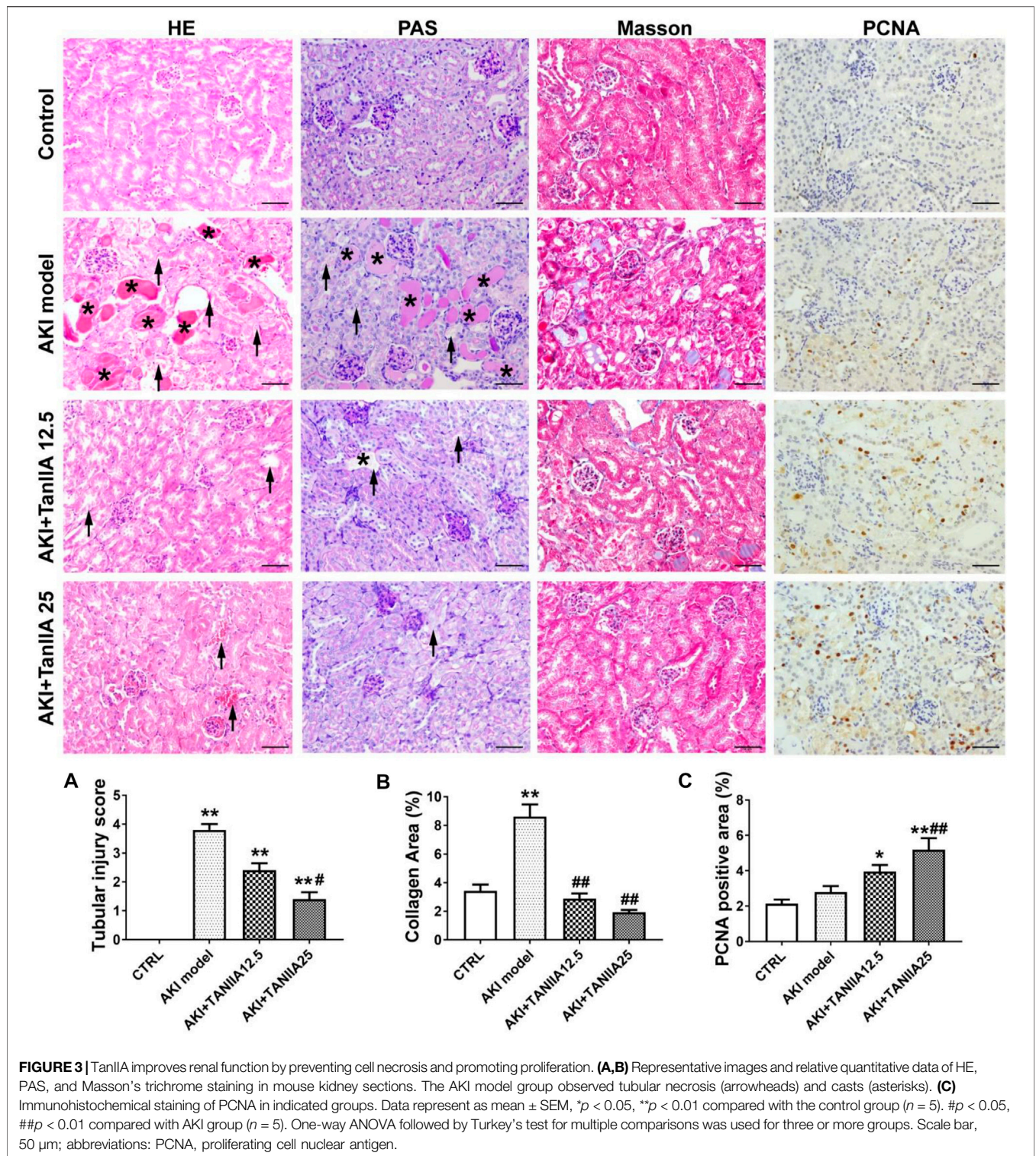
interfering RNA (siRNA) or the control siRNA. pGL4.32 [luc2P/NF- κ B-RE/Hygro], pCMV6-entry or pCMV6-XL4-hPXR, and pRL-TK control vector were transfected into the cells. HK-2 cells were stimulated by TNF- α (20 ng/ml) to activate NF- κ B signaling. As shown in **Figure 6C**, the pro-inflammatory cytokine TNF- α had significantly induced the luciferase activity of NF- κ B. When compared to the groups treated with TNF- α alone, TanIIA significantly reduced TNF- α -stimulated NF- κ B luciferase expression. In cells treated with TanIIA and stimulated by TNF- α (TNF- α + TanIIA), NF- κ B luciferase activities were significantly reduced in cells cotransfected with human PXR plasmid (pCMV6-XL4-hPXR). The result had suggested TanIIA repressed PXR-mediated NF- κ B activity. Besides, in HK-2 cells stimulated by TNF- α , immunofluorescence staining also revealed an inhibitory effect of TanIIA treatment on nuclear translocation of NF- κ B p65, suggesting TanIIA alleviated renal inflammation by repressing the activation of NF- κ B signaling (**Figure 6D**).

Interaction and Binding Mode of TanIIA and PXR

RMSD values are mainly used for analyzing the stability of protein and predicting conformational changes of the

protein. RMSD values depend upon the binding interaction and energy between the protein and ligand. The optimized protein has the lowest RMSD values (Carugo and Pongor, 2001). Generally, an RMSD value less than 1Å represents good reproduction of the correct pose. The molecular interactions like hydrogen bonds (H-bonds), hydrophobic interactions (such as π - π interaction and electrostatic interaction), *Van der Waals* interaction, and ionic bonds are also playing an important role in assessing the reliability of results and the binding stability between two modules (Patil et al., 2010).

TanIIA (chemical and 3D structure are shown in **Figures 7A,B**) could be docked into the active sites (binding pocket with LBD) of PXR (PDB ID: 1SKX). Inside the binding pocket, PXR consists of an endogenous ligand that had been confirmed as a PXR agonist. This ligand was used as a reference confirmation to compare docked TanIIA (**Figure 7C**). The RMSD of PXR (PDB ID: 1SKX) was 0.6720 Å (**Table 1**). Therefore, CDOCKER program was performed to analyze the interactions and binding features of PXR and TanIIA. Inside the binding pocket, TanIIA was surrounded by amino acids of the PXR protein (1SKX). Amino acids SER²⁴⁷ and GLN²⁸⁵ have formed H-bonds, and PHE²⁸⁸ and TRP²⁹⁹ formed π - π interactions between TanIIA and PXR (**Figure 7D**).



DISCUSSION

Acute kidney dysfunction impairs the essential physiological homeostasis of the body. Although the kidneys have the remarkable ability to regenerate, progressive inflammation may

eventually trigger renal fibrosis and lead to CKD (Gu et al., 2021). *Salvia miltiorrhiza* and its active compounds have been reported to have anti-inflammatory effects in the kidney disease (Gao et al., 2018). However, the role of *Salvia miltiorrhiza* in AKI awaits to be explored.

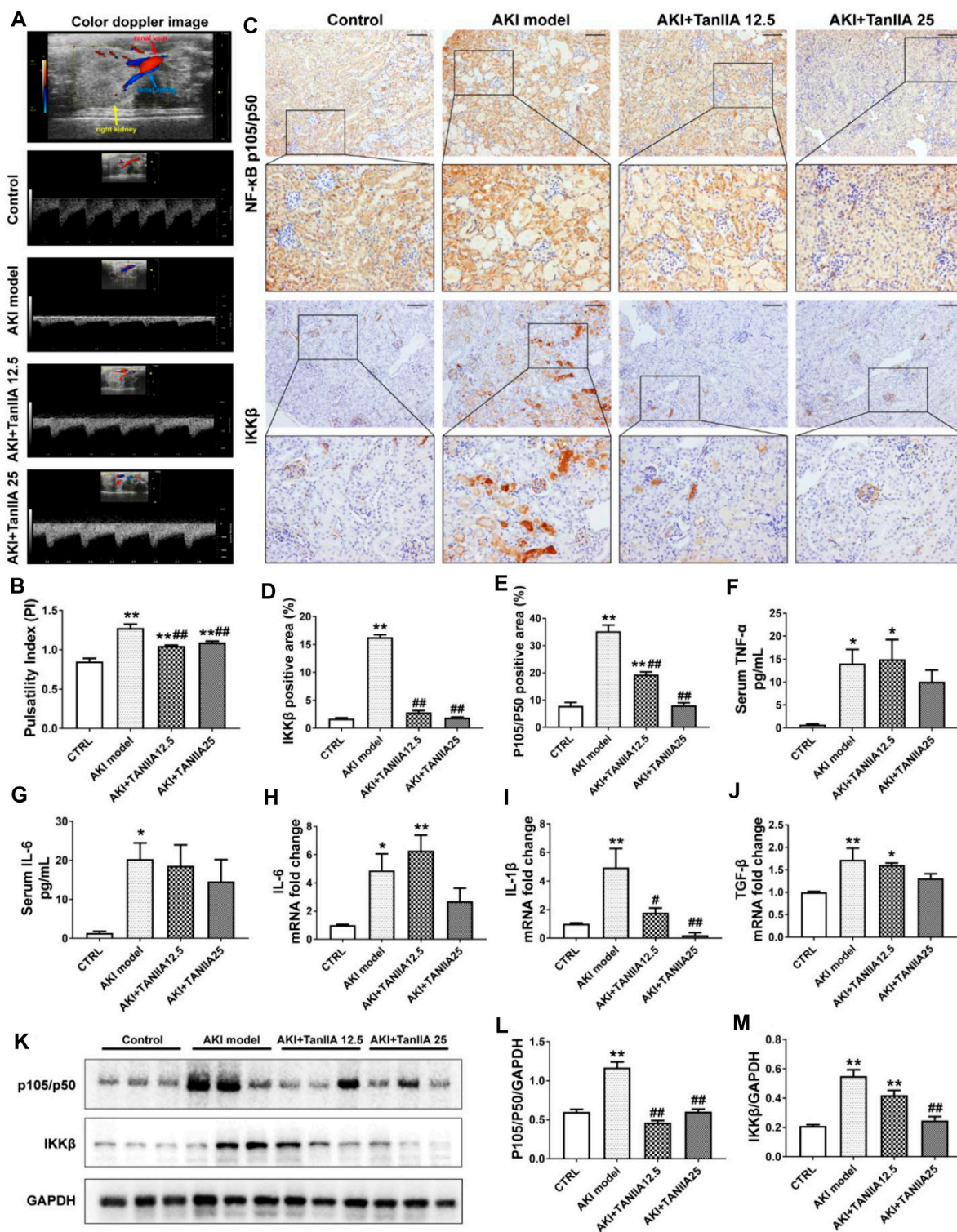
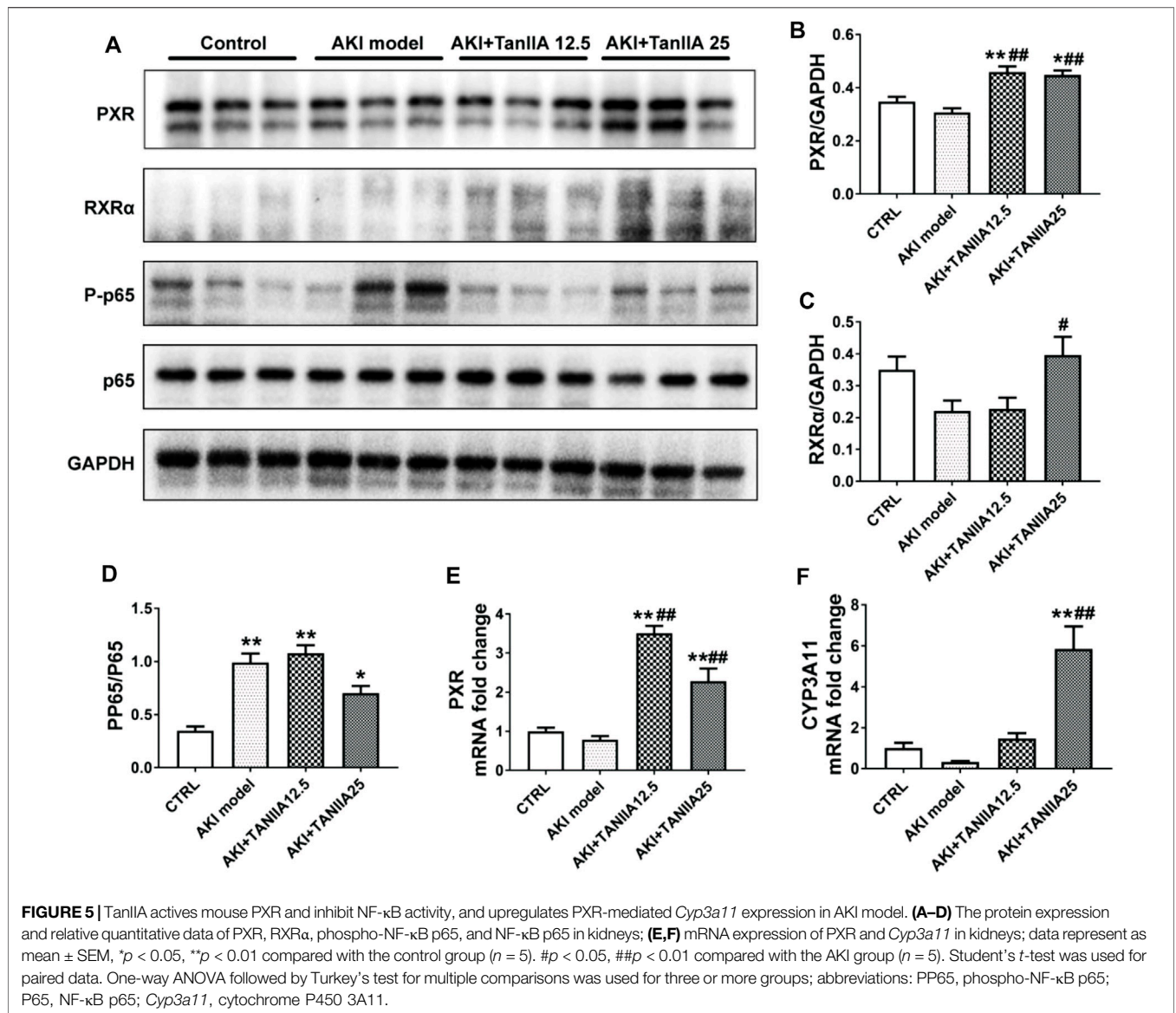


FIGURE 4 | TanIIA improves renal artery blood flow, reduces pro-inflammatory cytokine production, and inhibits the activation of NF-κB signaling. **(A,B)** Representative image of renal vasculature with color Doppler in a mouse kidney (right) and representative bar chart of pulsatility index (PI) in mice. **(C-E)** Immunohistochemical staining of NF-κB p105/p50 and IKKβ and relative quantitative data in indicated groups; **(F,G)** ELISA bar chart representing serum level of TNF-α and IL-6. **(H-J)** mRNA level of IL-6, IL-1β, and TGF-β in the kidney; **(K-M)** Protein expression and relative quantitative data of NF-κB p105/p50 and IKKβ. Data represent as mean ± SEM, **p* < 0.05, ***p* < 0.01 compared with the control group (*n* = 5). #*p* < 0.05, ##*p* < 0.01 compared with AKI group (*n* = 5). One-way ANOVA followed by Turkey's test for multiple comparisons was used for three or more groups. Scale bar, 50 μm; abbreviations: IKKβ, inhibitor of kappa B kinase beta; TNF-α, tumor necrosis factor-alpha; IL-6, interleukin-6; IL-1β, interleukin-1 β; TGF-β, transforming growth factor-β.

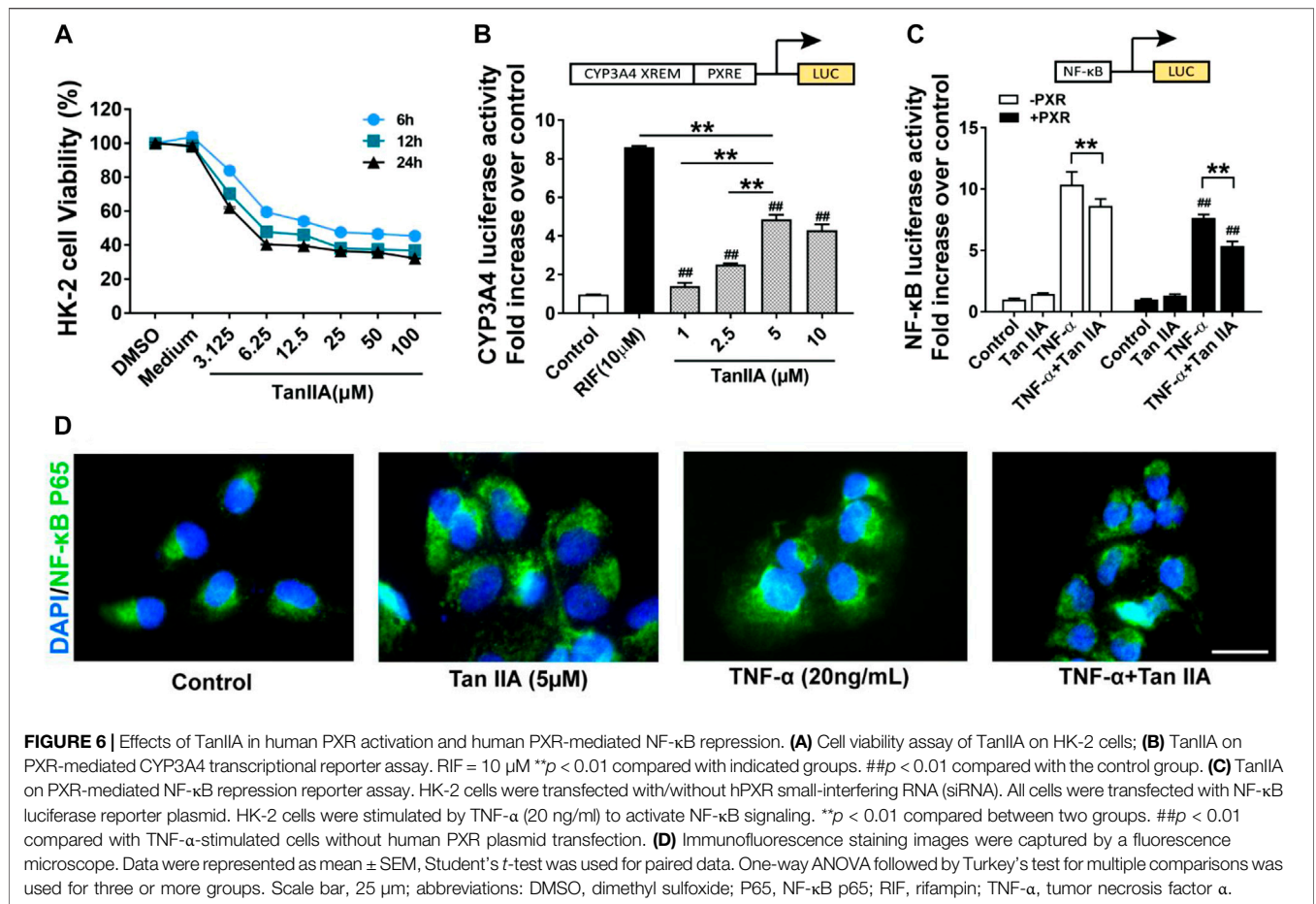


This study demonstrated the potential therapeutic role of *Salvia miltiorrhiza* and its bioactive compound TanIIA in AKI. Network pharmacological analysis shows a *Salvia miltiorrhiza*-targeted network in AKI, suggesting that the nuclear receptor family could be one of the significant targets. The study using cisplatin-induced AKI mice demonstrates that TanIIA treatment restores renal function in alleviating AKI-induced tubular necrosis and promoting cell proliferation. The production of pro-inflammatory cytokines and interstitial collagen accumulation is reduced by TanIIA treatment. Better perfusion on renal artery blood supply during the acute phase of kidney injury is also observed by color Doppler-based sonographic assessment in AKI mice treated with TanIIA.

Mechanistically, the present study has demonstrated that PXR activation improves renal function in AKI. The finding is consistent with previous findings, Luan *et al.* suggested that PXR activation may protect TECs from apoptosis in AKI by

regulating the PI3K/AKT signaling (Luan *et al.*, 2021); Yu *et al.* determined that PXR targeted AKR1B7 to improve mitochondrial metabolism and restored renal function in AKI (Yu *et al.*, 2020). The renal protective effect of TanIIA is dependent on PXR-mediated NF-κB repression. The PXR/NF-κB luciferase reporter assays suggest the role of TanIIA in reducing TNF-α-induced NF-κB activation in a PXR-dependent manner. As for molecular docking, the crystal structure of PXR enables computational investigations on protein–ligand sites and binding modes. We study the entry of TanIIA and its binding inside the PXR cavity. TanIIA stabilizes a binding geometry by forming H-bonds with amino acids SER²⁴⁷ and GLN²⁸⁵ and forming π–π interactions PHE²⁸⁸ and TRP²⁹⁹ with PXR. Molecular docking studies have provided evidence on the interaction and binding modes between TanIIA and PXR.

Previous studies have demonstrated a key role of PXR in inflammatory diseases (Ye *et al.*, 2016; Huang *et al.*, 2018; Klepsch



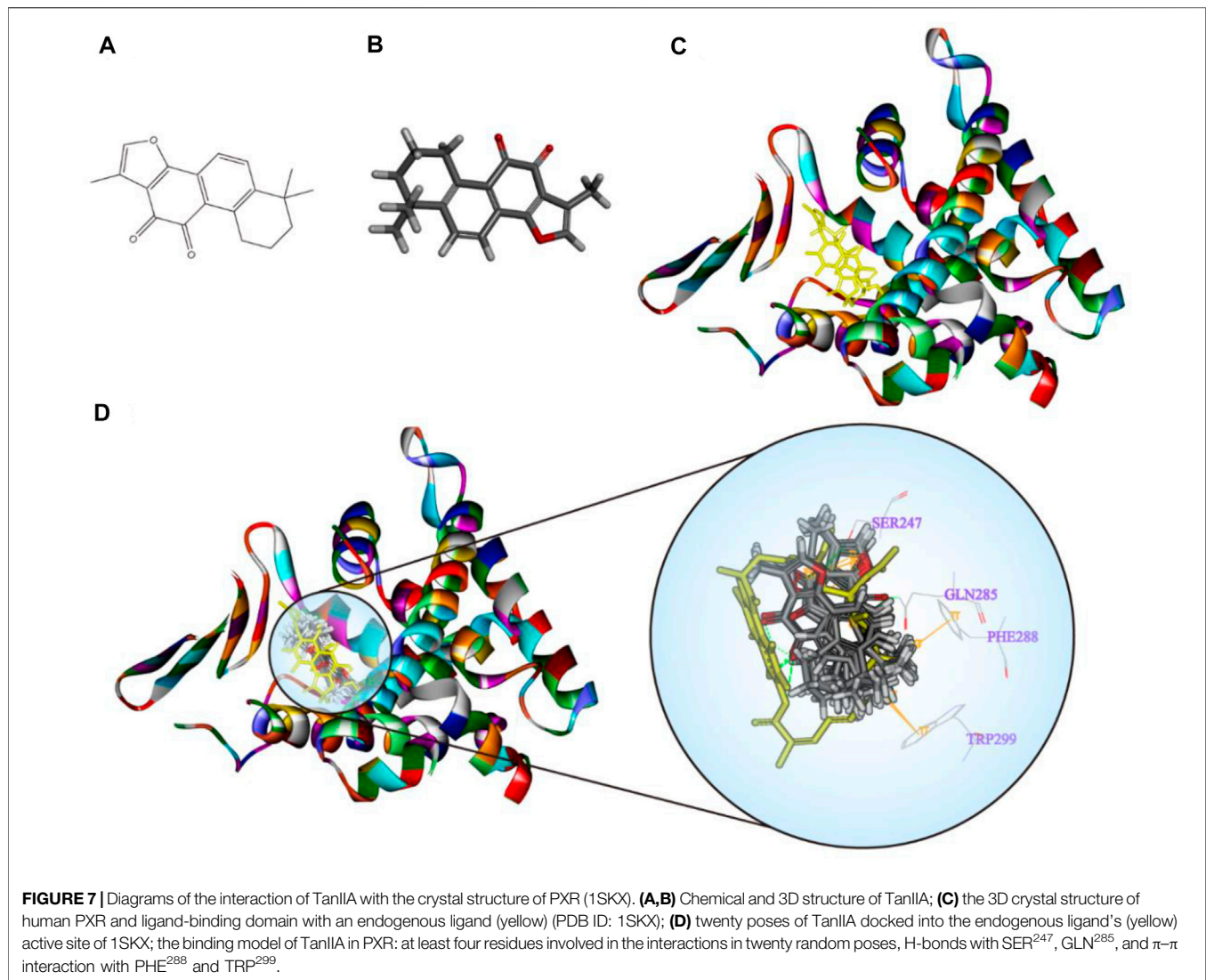
et al., 2019). PXR inhibits NF-κB activation to constrain inflammatory response (Deuring et al., 2019; Ren et al., 2019; Okamura et al., 2020). Although substantial PXR-activating xenobiotics have been reported to exert immunosuppressive effects (Wallace et al., 2010; Kittayaruksakul et al., 2013; Zhang J. et al., 2015; Rosette et al., 2019), the human PXR agonist rifampin is not an ideal choice for anti-inflammation treatment due to its adverse effects. The herbal PXR activators such as St. John's Wort and *Schisandra sphenanthera* (Wuweizi) have been used for a long time which may serve as a beneficial alternative medicine for inflammatory diseases (Mu et al., 2006; Yan et al., 2021). TanIIA is a bioactive compound derived from the root of *Salvia miltiorrhiza* and has been demonstrated as a PXR activator in various diseases (Yu et al., 2009; Zhang et al., 2015a; Zhang et al., 2015b; Zhu et al., 2017; Liu et al., 2020). However, PXR has shown a high degree of cross-species diversity due to the unusually divergent PXR LBD across species. Therefore, PXR of different species may respond diversely to the same ligand. For example, pregnenolone-16a-carbonitrile (PCN) is a potent agonist of mouse PXR but a poor activator of human PXR, and vice versa (Lecluyse, 2001). In this study, TanIIA activates both human and mouse PXR and induces the transcription of their target genes, CYP3A4 and *Cyp3a11*. The mouse model of AKI and NF-κB luciferase reporter assay in human HK-2 cells has indicated that TanIIA inhibits the activation of NF-κB signaling and its target genes. Of note, TanIIA represses both human and mouse PXR-mediated NF-κB activation.

TABLE 1 | Validation of molecular docking algorithm (RMSD).

Protein	CDOCKER RMSD (Å)	Libdock RMSD (Å)
1SKY	0.6720	6.6084

These findings are similar to those in the published literature. It is reported that PXR activation constrains the activity of NF-κB signaling that PXR competes with NF-κB for GRIP1 (NF-κB coactivator) interaction (Okamura et al., 2019). Moreover, PXR could directly interact with NF-κB p65, which inhibited the translocation of NF-κB to the nuclear, thereby suppressing the downstream inflammatory response (Wahli, 2008; Zhang et al., 2019; Shao et al., 2021). All these findings have suggested a potential role of PXR/NF-κB signaling in AKI.

Our study has several limitations. We used the C57BL/6 mouse model to establish a cisplatin-induced AKI, instead of the humanized PXR, *Pxr*-null, and wild-type mouse to mimic the human PXR signaling. In addition, we used rifampin as a positive control in HK-2 cells to study how TanIIA affects PXR activity but failed to put PCN as a positive control in the mouse model. Further study is required to provide evidence concerning TanIIA activation to mouse PXR. Due to length limits, we focused on the *Salvia miltiorrhiza*-regulated



nuclear receptor family, while other signaling pathways may also serve as potential targets. Further investigation on the renal protective effects of *Salvia miltiorrhiza* is warranted.

CONCLUSION

In summary, the present study provides new insights into the renoprotective effect of *Salvia miltiorrhiza* and TanIIA in AKI. TanIIA may ameliorate renal inflammation by repressing PXR-mediated NF- κ B activation. The results also suggest TanIIA as a PXR activator against renal inflammation. Our study sheds light on the specific regulatory role of the PXR/NF- κ B signaling pathway in kidney pathogenesis, and PXR may serve as a potential target in AKI treatment.

DATA AVAILABILITY STATEMENT

The datasets presented in this study can be found in online repositories. The names of the repository/repositories and accession number(s) can be found in the article/**Supplementary Material**.

ETHICS STATEMENT

The animal study was reviewed and approved by The experimental procedures were approved by the Institutional Animal Care and Use Committee of Guangdong Provincial Hospital of Chinese Medicine (Approval No. 2020020).

AUTHOR CONTRIBUTIONS

Y-YG conducted the whole study, wrote, and revised the manuscript. J-YD conducted the animal study. MZ conducted the network pharmacologic study and revised the manuscript. HC and Y-QC conducted the renal ultrasonic study. Y-FW and FL helped to analyze the data and revised the manuscript. JZ and X-SL revised the manuscript. All authors contributed to the manuscript conception development, data collection and analysis, and discussion on the manuscript writing and revising.

FUNDING

This work was supported by the National Natural Science Foundation of China (No. 81903956), the China Postdoctoral Science Foundation (2021M690042), the

Project of Guangdong Province Administration of Traditional Chinese Medicine (No. 20201133), and the Basic and Applied Basic Research Project of Guangzhou Science and Technology Department (202102020011).

ACKNOWLEDGMENTS

The authors would like to thank Haibo Liu from the Chinese Academy of Medical Sciences for providing the aforementioned docking software and Wecomput Technology for providing computation consulting.

SUPPLEMENTARY MATERIAL

The Supplementary Material for this article can be found online at: <https://www.frontiersin.org/articles/10.3389/fphar.2022.860383/full#supplementary-material>

REFERENCES

- Bespalov, A., Wicke, K., and Castagné, V. (2020). Blinding and Randomization. *Handb Exp. Pharmacol.* 257, 81–100. doi:10.1007/164_2019_279
- Bindea, G., Mlecnik, B., Hackl, H., Charoentong, P., Tosolini, M., Kirilovsky, A., et al. (2009). ClueGO: a Cytoscape Plug-In to Decipher Functionally Grouped Gene Ontology and Pathway Annotation Networks. *Bioinformatics* 25, 1091–1093. doi:10.1093/bioinformatics/btp101
- Carugo, O., and Pongor, S. (2001). A Normalized Root-Mean-Square Distance for Comparing Protein Three-Dimensional Structures. *Protein Sci.* 10, 1470–1473. doi:10.1110/ps.690101
- Charan, J., and Kantharia, N. D. (2013). How to Calculate Sample Size in Animal Studies? *J. Pharmacol. Pharmacother.* 4, 303–306. doi:10.4103/0976-500X.119726
- Deuring, J. J., Li, M., Cao, W., Chen, S., Wang, W., De Haar, C., et al. (2019). Pregnane X Receptor Activation Constrains Mucosal NF- κ B Activity in Active Inflammatory Bowel Disease. *PLoS One* 14, e0221924. doi:10.1371/journal.pone.0221924
- Gao, H., Huang, L., Ding, F., Yang, K., Feng, Y., Tang, H., et al. (2018). Simultaneous Purification of Dihydrotanshinone, Tanshinone I, Cryptotanshinone, and Tanshinone IIA from *Salvia Miltiorrhiza* and Their Anti-inflammatory Activities Investigation. *Sci. Rep.* 8, 8460. doi:10.1038/s41598-018-26828-0
- Gu, Y. Y., Chen, M. H., May, B. H., Liao, X. Z., Liu, J. H., Tao, L. T., et al. (2018). Matrine Induces Apoptosis in Multiple Colorectal Cancer Cell Lines *In Vitro* and Inhibits Tumour Growth with Minimum Side Effects *In Vivo* via Bcl-2 and Caspase-3. *Phytomedicine* 51, 214–225. doi:10.1016/j.phymed.2018.10.004
- Gu, Y. Y., Dou, J. Y., Huang, X. R., Liu, X. S., and Lan, H. Y. (2021). Transforming Growth Factor- β and Long Non-coding RNA in Renal Inflammation and Fibrosis. *Front. Physiol.* 12, 684236. doi:10.3389/fphys.2021.684236
- Guo, R., Li, L., Su, J., Li, S., Duncan, S. E., Liu, Z., et al. (2020). Pharmacological Activity and Mechanism of Tanshinone IIA in Related Diseases. *Drug Des. Devel Ther.* 14, 4735–4748. doi:10.2147/DDDT.S266911
- He, L., Zhou, X., Huang, N., Li, H., Li, T., Yao, K., et al. (2017). Functions of Pregnane X Receptor in Self-Detoxification. *Amino Acids* 49, 1999–2007. doi:10.1007/s00726-017-2435-0
- Hogle, B. C., Guan, X., Folan, M. M., and Xie, W. (2018). PXR as a Mediator of Herb-Drug Interaction. *J. Food Drug Anal.* 26, S26–s31. doi:10.1016/j.jfda.2017.11.007
- Hoste, E. A., Bagshaw, S. M., Bellomo, R., Cely, C. M., Colman, R., Cruz, D. N., et al. (2015). Epidemiology of Acute Kidney Injury in Critically Ill Patients: the Multinational AKI-EPI Study. *Intensive Care Med.* 41, 1411–1423. doi:10.1007/s00134-015-3934-7
- Huang, H., Wang, H., Sinz, M., Zockler, M., Staudinger, J., Redinbo, M. R., et al. (2007). Inhibition of Drug Metabolism by Blocking the Activation of Nuclear Receptors by Ketoconazole. *Oncogene* 26, 258–268. doi:10.1038/sj.onc.1209788
- Huang, K., Mukherjee, S., Desmarais, V., Albanese, J. M., Rafti, E., Draghi Ii, A., et al. (2018). Targeting the PXR-TLR4 Signaling Pathway to Reduce Intestinal Inflammation in an Experimental Model of Necrotizing Enterocolitis. *Pediatr. Res.* 83, 1031–1040. doi:10.1038/pr.2018.14
- Jiang, C., Shao, Q., Jin, B., Gong, R., Zhang, M., and Xu, B. (2015). Tanshinone IIA Attenuates Renal Fibrosis after Acute Kidney Injury in a Mouse Model through Inhibition of Fibrocytes Recruitment. *Biomed. Res. Int.* 2015, 867140. doi:10.1155/2015/867140
- Kelahan, L. C., Desser, T. S., Troxell, M. L., and Kamaya, A. (2019). Ultrasound Assessment of Acute Kidney Injury. *Ultrasound Q.* 35, 173–180. doi:10.1097/RUQ.0000000000000389
- Kellum, J. A., Romagnani, P., Ashuntantang, G., Ronco, C., Zarbock, A., and Anders, H. J. (2021). Acute Kidney Injury. *Nat. Rev. Dis. Primers* 7, 52. doi:10.1038/s41572-021-00284-z
- Kittayaruksakul, S., Zhao, W., Xu, M., Ren, S., Lu, J., Wang, J., et al. (2013). Identification of Three Novel Natural Product Compounds that Activate PXR and CAR and Inhibit Inflammation. *Pharm. Res.* 30, 2199–2208. doi:10.1007/s11095-013-1101-9
- Klepsch, V., Moschen, A. R., Tilg, H., Baier, G., and Hermann-Kleiter, N. (2019). Nuclear Receptors Regulate Intestinal Inflammation in the Context of IBD. *Front. Immunol.* 10, 1070. doi:10.3389/fimmu.2019.01070
- Lecluyse, E. L. (2001). Pregnane X Receptor: Molecular Basis for Species Differences in CYP3A Induction by Xenobiotics. *Chem. Biol. Interact* 134, 283–289. doi:10.1016/s0009-2797(01)00163-6
- Lee, H. J., Pyo, M. C., Shin, H. S., Ryu, D., and Lee, K. W. (2018). Renal Toxicity through AhR, PXR, and Nrf2 Signaling Pathway Activation of Ochratoxin A-Induced Oxidative Stress in Kidney Cells. *Food Chem. Toxicol.* 122, 59–68. doi:10.1016/j.fct.2018.10.004
- Liu, T. L., Zhang, L. N., Gu, Y. Y., Lin, M. G., Xie, J., Chen, Y. L., et al. (2020). The Synergistic Antitumor Effect of Tanshinone IIA Plus Adriamycin on Human Hepatocellular Carcinoma Xenograft in BALB/C Nude Mice and Their Influences on Cytochrome P450 CYP3A4 *In Vivo*. *Adv. Med.* 2020, 6231751. doi:10.1155/2020/6231751
- Liu, Y. H., Mo, S. L., Bi, H. C., Hu, B. F., Li, C. G., Wang, Y. T., et al. (2011). Regulation of Human Pregnane X Receptor and its Target Gene Cytochrome P450 3A4 by Chinese Herbal Compounds and a Molecular Docking Study. *Xenobiotica* 41, 259–280. doi:10.3109/00498254.2010.537395
- Luan, Z., Wei, Y., Huo, X., Sun, X., Zhang, C., Ming, W., et al. (2021). Pregnane X Receptor (PXR) Protects against Cisplatin-Induced Acute Kidney Injury in Mice. *Biochim. Biophys. Acta Mol. Basis Dis.* 1867, 165996. doi:10.1016/j.bbdis.2020.165996

- Ma, X. H., Ma, Y., Tang, J. F., He, Y. L., Liu, Y. C., Ma, X. J., et al. (2015). The Biosynthetic Pathways of Tanshinones and Phenolic Acids in *Salvia Miltiorrhiza*. *Molecules* 20, 16235–16254. doi:10.3390/molecules200916235
- Markó, L., Vigolo, E., Hinze, C., Park, J. K., Roël, G., Balogh, A., et al. (2016). Tubular Epithelial NF-κB Activity Regulates Ischemic AKI. *J. Am. Soc. Nephrol.* 27, 2658–2669. doi:10.1681/ASN.2015070748
- Mu, Y., Zhang, J., Zhang, S., Zhou, H. H., Toma, D., Ren, S., et al. (2006). Traditional Chinese Medicines Wu Wei Zi (*Schisandra Chinensis* Bail) and Gan Cao (*Glycyrrhiza Uralensis* Fisch) Activate Pregnane X Receptor and Increase Warfarin Clearance in Rats. *J. Pharmacol. Exp. Ther.* 316, 1369–1377. doi:10.1124/jpet.105.094342
- Okamura, M., Shizu, R., Hosaka, T., Sasaki, T., and Yoshinari, K. (2019). Possible Involvement of the Competition for the Transcriptional Coactivator Glucocorticoid Receptor-Interacting Protein 1 in the Inflammatory Signal-dependent Suppression of PXR-Mediated CYP3A Induction *In Vitro*. *Drug Metab. Pharmacokin.* 34, 272–279. doi:10.1016/j.dmpk.2019.04.005
- Okamura, M., Shizu, R., Abe, T., Kodama, S., Hosaka, T., Sasaki, T., et al. (2020). PXR Functionally Interacts with NF-κB and AP-1 to Downregulate the Inflammation-Induced Expression of Chemokine CXCL2 in Mice. *Cells* 9, 2296. doi:10.3390/cells9102296
- Okumura, K., Matsumoto, J., Iwata, Y., Yoshida, K., Yoneda, N., Ogi, T., et al. (2018). Evaluation of Renal Oxygen Saturation Using Photoacoustic Imaging for the Early Prediction of Chronic Renal Function in a Model of Ischemia-Induced Acute Kidney Injury. *PLoS One* 13, e0206461. doi:10.1371/journal.pone.0206461
- Oladimeji, P. O., and Chen, T. (2018). PXR: More Than Just a Master Xenobiotic Receptor. *Mol. Pharmacol.* 93, 119–127. doi:10.1124/mol.117.110155
- Ozkok, A., and Edelstein, C. L. (2014). Pathophysiology of Cisplatin-Induced Acute Kidney Injury. *Biomed. Res. Int.* 2014, 967826. doi:10.1155/2014/967826
- Patil, R., Das, S., Stanley, A., Yadav, L., Sudhakar, A., and Varma, A. K. (2010). Optimized Hydrophobic Interactions and Hydrogen Bonding at the Target-Ligand Interface Leads the Pathways of Drug-Designing. *PLoS One* 5, e12029. doi:10.1371/journal.pone.0012029
- Ren, Y., Yue, B., Ren, G., Yu, Z., Luo, X., Sun, A., et al. (2019). Activation of PXR by Alantolactone Ameliorates DSS-Induced Experimental Colitis via Suppressing NF-κB Signaling Pathway. *Sci. Rep.* 9, 16636. doi:10.1038/s41598-019-53305-z
- Rosette, C., Agan, F. J., Rosette, N., Moro, L., Mazzetti, A., Hassan, C., et al. (2019). Rifamycin SV Exhibits strong Anti-inflammatory *In vitro* Activity through Pregnane X Receptor Stimulation and NFκB Inhibition. *Drug Metab. Pharmacokin.* 34, 172–180. doi:10.1016/j.dmpk.2019.01.002
- Ru, J., Li, P., Wang, J., Zhou, W., Li, B., Huang, C., et al. (2014). TC MSP: A Database of Systems Pharmacology for Drug Discovery from Herbal Medicines. *J. Cheminform* 6, 13. doi:10.1186/1758-2946-6-13
- Scholz, H., Boivin, F. J., Schmidt-Ott, K. M., Bachmann, S., Eckardt, K. U., Scholl, U. I., et al. (2021). Kidney Physiology and Susceptibility to Acute Kidney Injury: Implications for Renoprotection. *Nat. Rev. Nephrol.* 17, 335–349. doi:10.1038/s41581-021-00394-7
- Schrezenmeier, E. V., Barasch, J., Budde, K., Westhoff, T., and Schmidt-Ott, K. M. (2017). Biomarkers in Acute Kidney Injury - Pathophysiological Basis and Clinical Performance. *Acta Physiol. (Oxf)* 219, 554–572. doi:10.1111/apha.12764
- Shao, Y. Y., Guo, Y., Feng, X. J., Liu, J. J., Chang, Z. P., Deng, G. F., et al. (2021). Oridonin Attenuates TNBS-Induced Post-inflammatory Irritable Bowel Syndrome via PXR/NF-κB Signaling. *Inflammation* 44, 645–658. doi:10.1007/s10753-020-01364-0
- Song, N., Thaiss, F., and Guo, L. (2019). NFκB and Kidney Injury. *Front. Immunol.* 10, 815. doi:10.3389/fimmu.2019.00815
- The UniProt Consortium (2018). UniProt: the Universal Protein Knowledgebase. *Nucleic Acids Res.* 46, 2699. doi:10.1093/nar/gky092
- Velenosi, T. J., Feere, D. A., Sohi, G., Hardy, D. B., and Urquhart, B. L. (2014). Decreased Nuclear Receptor Activity and Epigenetic Modulation Associates with Down-Regulation of Hepatic Drug-Metabolizing Enzymes in Chronic Kidney Disease. *Faseb j* 28, 5388–5397. doi:10.1096/fj.14-258780
- Von Mering, C., Huynen, M., Jaeggi, D., Schmidt, S., Bork, P., and Snel, B. (2003). STRING: a Database of Predicted Functional Associations between Proteins. *Nucleic Acids Res.* 31, 258–261. doi:10.1093/nar/gkg034
- Wahli, W. (2008). A Gut Feeling of the PXR, PPAR and NF-κB Connection. *J. Intern. Med.* 263, 613–619. doi:10.1111/j.1365-2796.2008.01951.x
- Wallace, K., Cowie, D. E., Constantinou, D. K., Hill, S. J., Tjelle, T. E., Axon, A., et al. (2010). The PXR Is a Drug Target for Chronic Inflammatory Liver Disease. *J. Steroid Biochem. Mol. Biol.* 120, 137–148. doi:10.1016/j.jsbmb.2010.04.012
- Watanabe, A., Marumo, T., Kawarazaki, W., Nishimoto, M., Ayuzawa, N., Ueda, K., et al. (2018). Aberrant DNA Methylation of Pregnane X Receptor Underlies Metabolic Gene Alterations in the Diabetic Kidney. *Am. J. Physiol. Ren. Physiol* 314, F551–F560. doi:10.1152/ajprenal.00390.2017
- Yan, T., Luo, Y., Xia, Y., Hamada, K., Wang, Q., Yan, N., et al. (2021). St. John's Wort Alleviates Dextran Sodium Sulfate-Induced Colitis through Pregnane X Receptor-dependent NFκB Antagonism. *Faseb j* 35, e21968. doi:10.1096/fj.202001098R
- Ye, N., Wang, H., Hong, J., Zhang, T., Lin, C., and Meng, C. (2016). PXR Mediated Protection against Liver Inflammation by Ginkgolide A in Tetrachloromethane Treated Mice. *Biomol. Ther. (Seoul)* 24, 40–48. doi:10.4062/biomolther.2015.077
- Yu, C., Ye, S., Sun, H., Liu, Y., Gao, L., Shen, C., et al. (2009). PXR-mediated Transcriptional Activation of CYP3A4 by Cryptotanshinone and Tanshinone IIA. *Chem. Biol. Interact* 177, 58–64. doi:10.1016/j.cbi.2008.08.013
- Yu, X., Xu, M., Meng, X., Li, S., Liu, Q., Bai, M., et al. (2020). Nuclear Receptor PXR Targets AKR1B7 to Protect Mitochondrial Metabolism and Renal Function in AKI. *Sci. Transl. Med.* 12, eaay7591. doi:10.1126/scitranslmed.aay7591
- Zhang, J., Cai, Z., Yang, M., Tong, L., and Zhang, Y. (2020). Inhibition of Tanshinone IIA on Renin Activity Protected against Osteoporosis in Diabetic Mice. *Pharm. Biol.* 58, 219–224. doi:10.1080/13880209.2020.1738502
- Zhang, J., Ding, L., Wang, B., Ren, G., Sun, A., Deng, C., et al. (2015). Notoginsenoside R1 Attenuates Experimental Inflammatory Bowel Disease via Pregnane X Receptor Activation. *J. Pharmacol. Exp. Ther.* 352, 315–324. doi:10.1124/jpet.114.218750
- Zhang, J., Zhao, Z., Bai, H., Wang, M., Jiao, L., Peng, W., et al. (2019). Genetic Polymorphisms in PXR and NF-κB1 Influence Susceptibility to Anti-tuberculosis Drug-Induced Liver Injury. *PLoS One* 14, e0222033. doi:10.1371/journal.pone.0222033
- Zhang, X., Ma, Z., Liang, Q., Tang, X., Hu, D., Liu, C., et al. (2015a). Tanshinone IIA Exerts Protective Effects in a LCA-Induced Cholestatic Liver Model Associated with Participation of Pregnane X Receptor. *J. Ethnopharmacol* 164, 357–367. doi:10.1016/j.jep.2015.01.047
- Zhang, X., Wang, Y., Ma, Z., Liang, Q., Tang, X., Hu, D., et al. (2015b). Tanshinone IIA Ameliorates Dextran Sulfate Sodium-Induced Inflammatory Bowel Disease via the Pregnane X Receptor. *Drug Des. Devel Ther.* 9, 6343–6362. doi:10.2147/DDDT.S79388
- Zhu, H., Chen, Z., Ma, Z., Tan, H., Xiao, C., Tang, X., et al. (2017). Tanshinone IIA Protects Endothelial Cells from H₂O₂-Induced Injuries via PXR Activation. *Biomol. Ther. (Seoul)* 25, 599–608. doi:10.4062/biomolther.2016.179

Conflict of Interest: The authors declare that the research was conducted in the absence of any commercial or financial relationships that could be construed as a potential conflict of interest.

Publisher's Note: All claims expressed in this article are solely those of the authors and do not necessarily represent those of their affiliated organizations, or those of the publisher, the editors, and the reviewers. Any product that may be evaluated in this article, or claim that may be made by its manufacturer, is not guaranteed or endorsed by the publisher.

Copyright © 2022 Dou, Zhang, Cen, Chen, Wu, Lu, Zhou, Liu and Gu. This is an open-access article distributed under the terms of the Creative Commons Attribution License (CC BY). The use, distribution or reproduction in other forums is permitted, provided the original author(s) and the copyright owner(s) are credited and that the original publication in this journal is cited, in accordance with accepted academic practice. No use, distribution or reproduction is permitted which does not comply with these terms.